LRP 563/96 December 1996

G2DEM: A PARALLEL TWO-DIMENSIONAL ELECTROMAGNETIC PIC CODE FOR THE STUDY OF ELECTRON-CYCLOTRON INSTABILITIES OF RELATIVISTIC ELECTRON BEAMS IN CYLINDRICAL CAVITIES

G. Jost, T.M. Tran, K. Appert, S. Wüthrich

submitted for publication to
Computer Physics Communications

G2DEM : A parallel two-dimensional electromagnetic PIC code for the study of electron-cyclotron instabilities of relativistic electron beams in cylindrical cavities

G. Jost [a], T. M. Tran [a], K. Appert [a], S. Wüthrich [b]

[a] *Centre de Recherches en Physique des Plasmas, Association Euratom-Confédération Suisse, Ecole Polytechnique Fédérale de Lausanne, CH-1015 Lausanne, Switzerland*

[b] *CRAY Research, PATP/PSE, EPFL, CH-1015 Lausanne, Switzerland*

A two-dimensional PIC code aimed at the investigation of electron-cyclotron beam instabilities in gyrotrons and their effects on the beam quality is presented. The code is based on recently developed techniques for handling charge conservation and open boundaries and uses an electromagnetic field which is decomposed in its transverse magnetic (TM) and electric (TE) components. The code has been implemented on the massively parallel computer CRAY T3D, and on the CRAY Y-MP.

Key words: Gyrotron ; Electromagnetic-PIC simulation ; Electron -cyclotron instabilities ; Current assignment ; Open boundaries

PROGRAM SUMMARY

Title of program: G2DEM

Catalog number:

Program obtainable from: CPC Program Library, Queen's University of Belfast, N. Ireland

Licensing provisions: none

Computer for which the program is designed and others on which it is operable: CRAY T3D, CRAY Y-MP

Computer: T3D MC256-8, CRAY Y-MP/M94; *Installation:* Ecole Polytechnique Fédérale de Lausanne

Operating systems under which the program has been tested: UNICOS

Program language used: FORTRAN 77

Compiler options: T3D : with SHMEM routines cf77 -dp -DT3D -DSHMEM -I. -I/usr/include/mpp -lpvm3, without SHMEM routines cf77 -dp -DT3D -I. -I/usr/include/mpp -lpvm3 ; Y-MP : cf77 -dp -DYMP -Zv -I.

Memory required to execute with typical data: On the Y-MP, the memory required is proportional to the number of particles going from 8 MWords for 25000 particles to 32 MWords for 100000 particles.

No. of bits in a word: 64

No. of processors used: from 8 to 32 on the T3D

No. of lines in distributed program, including test data, etc: 9996

Distribution format: ASCII

Keywords: Gyrotron; Electromagnetic-PIC simulation; Electron-cyclotron instabilities; Current assignment; Open boundaries

Nature of physical problem

G2DEM (Gyrotron 2 Dimensions ElectroMagnetic) solves Maxwell's equations and the relativistic equations of motion for an annular electron beam in an axisymmetric cylindrical cavity (r, z) open at both ends. This program is used to determine the effects of electron-cyclotron instabilities (electrostatic and electromagnetic) on the velocity distribution of the beam. This is of practical interest, because the best gyrotron efficiency is obtained with monochromatic beams and any beam degradation, leading to a loss of monochromaticity in either energy or velocity pitch angle, lowers it [1].

Method of solution

G2DEM is a particle-in-cell (PIC) code [2,3], in which the Maxwell equations are discretized by the finite element method. The current carried by a particle is obtained from a charge conserving assignment scheme called the Virtual Particle Method [4]. Open boundaries are treated by the method of the Perfectly Matched Layer [5]. On the CRAY T3D, the particles are distributed among the processors independently of their position and velocity, the electromagnetic field is updated in parallel, using a domain decomposition of the cavity [6].

Typical running time

The running time depends strongly on physical parameters like the length of the cavity and the beam current, which determine the number of particles and mesh points, and the saturation time, respectively. It is dominantly ($\approx$ 90 % of it) affected by the number of particles, each one requiring 35 μs per step and processor, and by the number of processors. Together, these two quantities determine the fraction of time spent in communication [6]. On a 16 processor T3D configuration, the provided test runs require less than 500 seconds wall clock time but spend most of it in communications. In contrast to this, useful production runs might need more than a day on the same computer configuration but loose 20% of the time in communication.

Unusual feature of the program

The code is written in standard FORTRAN 77 and its structure conforms to the prescriptions of the OLYMPUS system [7]. The T3D version uses the CRAY SHMEM [8] and the PVM message passing libraries [9]. It can, however, run with PVM routines alone if the SHMEM library is not be available. Plots are obtained with an independent graphics module, called READB. This module is included in the G2DEM package and uses the publically available graphics library Xgrafix [10].

References

[1] S. Alberti et al. Physics Fluids B2 (1990)1654

[2] C. K. Birdsall, A. B. Langdon, "Plasma Physics via Computer Simulation", Adam Hilger, New York, 1991.

[3] R. W. Hockney, J. W. Eastwood, "Computer Simulation Using Particles", Institute of Physics Publishing, Bristol, 1988.

[4] J. W. Eastwood, Computer Physics Communications 64 (1991) 252.

[5] J-P. Bérenger, Journal of Computational Physics 114 (1994) 185.

[6] G. Jost, T. M. Tran, K. Appert and S. Wüthrich, "Effects of electron-cyclotron instabilities on gyrotron beam quality", accepted for publication in Computer Physics Communications.

[7] K. V. Roberts, Computer Physics Communications 7 (1974) 237.

[8] R. Barriuso, A. Knies, SHMEM User'Guide for Fortran, Cray Research Inc., Eagan, MN., August 15, 1994.

[9] G. A. Geist, A. L. Beguelin, J. J. Dongarra, R. J. Mancheck and V. S. Sunderam, PVM 3.0 User's Guide and Reference Manual, ORNL/TM-12187, 1993.

[10] V. Vahedi, J. P. Verboncoeur and P. Mirrashidi "Xgrafix library Version 1.1" University of California, Berkeley. Code and documentation are available through http://langmuir.eecs.berkeley.edu/pub/codes/Xgrafix.

LONG WRITE-UP

1 Introduction

The present code has been developed in support of the experimental R&D effort in quasioptical gyrotrons at the Centre de Recherches en Physique des Plasmas. In quasioptical gyrotron experiments, it had always been found that the efficiency for converting the relativistic electron beam energy into a well defined electromagnetic wave mode was substantially smaller than that predicted by theorical steady-state models [1]. The main ingredient in a theoretical efficiency estimate is the form of the velocity distribution of the beam electrons before the interaction with the electromagnetic wave in question. As it is practically impossible to obtain all the needed information from an experiment [2], PIC simulations can be very helpful in bridging the gaps in knowledge. Only by tight comparison between laboratory measurements and numerical results have we been able to explain plausibly the problems encountered in quasioptical gyrotrons [3].

This code has only been applied to gyrotrons, devices always driven by axisymmetric annular electron beams. The particles in the present numerical model will therefore never approach the symmetry axis, a fact which has implicitly been exploited by not considering problems connected with the axis. If the code should be used for the simulation of a solid particle beam some modifications will be needed to treat the particles near the axis correctly.

It would have demanded excessively large computer resources to try to model a complete gyrotron device with electron gun, beam tunnel, wave cavity and collector. We have here only modelled the beam tunnel where beam quality degrading electrostatic and electromagnetic instabilities can easily arise. A numerical experiment restricted to the beam tunnel can, however, only be meaningful when the excited electromagnetic waves can freely leave the computational domain. This has been achieved by using a recent method [4] for the treatment of computational boundaries open to electromagnetic waves. It has been shown that this method performs well in a PIC code [5, sec. 5].

The main characteristics of the code G2DEM have been described in a computational physics paper [5] dealing with the transverse magnetic polarization alone. To avoid repetition in the present paper, we extensively refer to the

former as paper I. Section, appendix and equation numbers preceded by "I" will refer to the respective item in reference [5].

The basic physical problem has been presented in Section I.2, the numerical treatment of the particle equations in Section I.3, the particle injection in Appendix I.B, the discretization of the equations governing the transverse magnetic (TM) polarization in Appendix I.A, the open boundaries in Section I.3, and the numerical implementation of G2DEM on a parallel computer in Section I.4. In the present paper, we treat the transverse electric (TE) polarization, and describe a few improvements of G2DEM not described in reference [5].

The structure of this write-up is therefore as follows. In Section 2, the physical problem is briefly reviewed and complemented. In Section 3, we present the discrete equations governing the TE polarization, and the treatment of boundaries for this polarization using Bérenger's technique of the perfectly matched layer [4]. In Section 4, the OLYMPUS structure of code and data is mentioned, and the most important information concerning input/output quantities and files are given. Section 4 also contains a short description of how the output data is post-processed with the graphics module READB.

2 Physical problem

The beam tunnel is modelled by an azimuthally symmetric cylindrical cavity (coordinates r, z, see fig.1) of radius R_w and length L_z which is open at $z = 0$ and $z = L_z$ (see Section I.2), and immersed in an external magnetic field $\vec{B}_0$, given by :

$$\vec{B}_0 = \begin{cases} b_0 \hat{e}_z & z < 0 \\ -\frac{1}{2} b_0 \tau r \hat{e}_r + b_0(1 + \tau z)\hat{e}_z & 0 \leq z \leq L_z \\ b_0(1 + \tau L_z)\hat{e}_z & L_z < z \end{cases} \tag{1}$$

where $\hat{e}_r$, $\hat{e}_z$ are the unit vectors in the cylindrical coordinates, and τ the constant taper of the magnetic field.

The beam electrons evolve according to the relativistic equations of motion, eqs.(I.1-2), whereas the electromagnetic field satisfies Maxwell's equations, which in this geometry can be separated into the TM,

$$\frac{\partial E_r}{\partial t} = -c^2 \frac{\partial B_\theta}{\partial z} - \frac{1}{\epsilon_0} j_r, \tag{2}$$

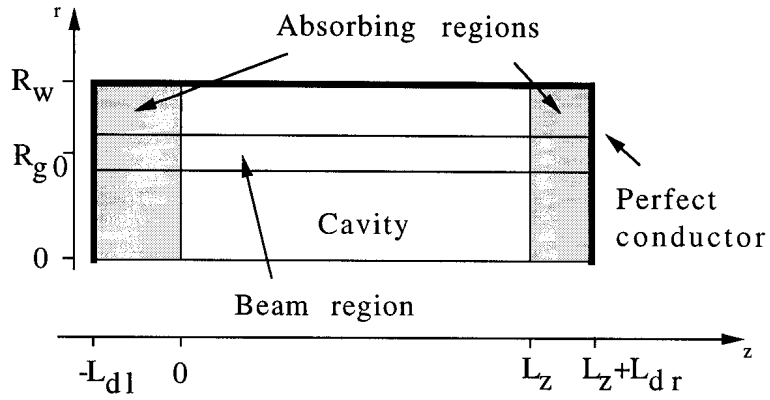

Fig. 1. Numerical model of the cavity representing the gyrotron beam tunnel.

$$\frac{\partial E_z}{\partial t} = c^2 \frac{1}{r}\frac{\partial}{\partial r}(rB_\theta) - \frac{1}{\epsilon_0} j_z, \tag{3}$$

$$\frac{\partial B_\theta}{\partial t} = -(\frac{\partial E_r}{\partial z} - \frac{\partial E_z}{\partial r}), \tag{4}$$

and the TE polarizations,

$$\frac{\partial E_\theta}{\partial t} = c^2(\frac{\partial B_r}{\partial z} - \frac{\partial B_z}{\partial r}) - \frac{1}{\epsilon_0} j_\theta, \tag{5}$$

$$\frac{\partial B_r}{\partial t} = \frac{\partial E_\theta}{\partial z}, \tag{6}$$

$$\frac{\partial B_z}{\partial t} = -\frac{1}{r}\frac{\partial}{\partial r}(rE_\theta). \tag{7}$$

Here ϵ_0 is the permittivity of vacuum and $\vec{j}$ is the current density.

3 Numerical scheme

All the equations used in the code are dimensionless. The applied normalization is shown in table 1 where the original physical quantities are denoted by the subscript ph and e, c, m and μ_0 have the usual meaning [6]. In the remainder of this paper, t, x, $\vec{B}$, $\vec{E}$ and $\vec{j}$ will denote the normalized quantities.

As the computational mesh and the integration of the particle equations are presented in Section I.3, we here only need to describe the generalization of the particle injection procedure of Appendix I.B, which allows the injection

Table 1
Normalization

Time	$t = eb_0/m * t_{ph}$
Position	$x = cm/eb_0 * x_{ph}$
Magnetic field	$\vec{B} = (1/b_0) * \vec{B}_{ph}$
Electric field	$\vec{E} = (1/b_0 c) * \vec{E}_{ph}$
Current	$\vec{j} = (\mu_0 mc/eb_0^2) * \vec{j}_{ph}$

of an electron beam having its guiding centers spread out radially. The initial guiding center of the particles injected between the times t^n and $t^{n+1} = t^n + \Delta t$ is now defined as :

$$R_g = R_{g_0}(1 + f_g \xi_g), \tag{8}$$

where R_{g_0} and f_g are the initial mean value and spread of the guiding centers, respectively. Their values are obtained from input (sec. 4.1). The quantity ξ_g is a random number between $-\frac{1}{2}$ and $\frac{1}{2}$. The radial position at time $t^{n+\frac{1}{2}}$, eq.(I.B.4) is now given by :

$$r^{n+\frac{1}{2}} = \sqrt{(R_g + r_L \sin\Theta)^2 + (r_L \cos\Theta)^2}, \tag{9}$$

where r_L is the gyroradius $|\frac{P_\perp}{-eb_0}|$ and Θ the gyroangle.

3.1 TE polarization

The two-dimensional (r, z) finite element representation of the electric and magnetic field can be obtained in a consistent way from the corresponding representations of the potentials ϕ and $\vec{A}$ [7]. In the present axisymmetric case, A_θ must be differentiable in both directions, r and z, and must therefore be at least linear in these directions. This can be achieved by choosing for A_θ a bilinear approximation. The finite element approximation for the electric and magnetic components of the TE polarization are then given by [7] :

$$E_\theta = \sum_{i=1}^{N_r+1} \sum_{j=1}^{N_z+1} E_{\theta i,j}\, \Lambda_i(r)\, \Lambda_j(z), \tag{10}$$

$$B_r = \sum_{i=1}^{N_r+1} \sum_{j=1}^{N_z} B_{r i,j+\frac{1}{2}}\, \Lambda_i(r)\, \Pi_{j+\frac{1}{2}}(z), \tag{11}$$

$$B_z = \sum_{i=1}^{N_r} \sum_{j=1}^{N_z+1} B_{z_{i+\frac{1}{2},j}} \Pi_{i+\frac{1}{2}}(r) \Lambda_j(z), \tag{12}$$

where Λ and Π are the triangle (piecewise linear) and the top hat (piecewise constant) finite element basis functions. In z direction, they are defined by :

$$\Lambda_j(z) = \begin{cases} \frac{z-z_{j-1}}{z_j-z_{j-1}} & z_{j-1} \le z \le z_j \\ \frac{z_{j+1}-z}{z_{j+1}-z_j} & z_j \le z \le z_{j+1} \\ 0 & \text{otherwise} \end{cases} \tag{13}$$

$$\Pi_{j+\frac{1}{2}}(z) = \begin{cases} 1 & z_j \le z \le z_{j+1} \\ 0 & \text{otherwise} \end{cases} \tag{14}$$

where z_j is the position of the meshpoint j. The functions $\Lambda(r)$ and $\Pi(r)$ are defined analogously. The quantities N_r and N_z in eqs. (10-12) denote the number of meshpoints along the r and z axis respectively (cp. Section I.3).

After lumping the mass matrix, and using an explicit time integration scheme [8], the normalized discrete equations become :

$$\begin{aligned} E_{\theta_{i,j}}^{n+1} &= E_{\theta_{i,j}}^{n} \\ &\quad + \Delta t \left(\frac{B_{r_{i,j+\frac{1}{2}}}^{n+\frac{1}{2}} - B_{r_{i,j-\frac{1}{2}}}^{n+\frac{1}{2}}}{z_{j+\frac{1}{2}} - z_{j-\frac{1}{2}}} - \frac{B_{z_{i+\frac{1}{2},j}}^{n+\frac{1}{2}} - B_{z_{i-\frac{1}{2},j}}^{n+\frac{1}{2}}}{r_{i+\frac{1}{2}} - r_{i-\frac{1}{2}}} \right) \\ &\quad - \Delta t \, j_{\theta_{i,j}}^{n+\frac{1}{2}}, \end{aligned} \tag{15}$$

$$\begin{aligned} B_{r_{i,j+\frac{1}{2}}}^{n+\frac{1}{2}} &= B_{r_{i,j+\frac{1}{2}}}^{n-\frac{1}{2}} \\ &\quad + \frac{\Delta t}{z_{j+1} - z_j} \left(E_{\theta_{i,j+1}}^{n+1} - E_{\theta_{i,j}}^{n+1} \right), \end{aligned} \tag{16}$$

$$\begin{aligned} B_{z_{i+\frac{1}{2},j}}^{n+\frac{1}{2}} &= B_{z_{i-\frac{1}{2},j}}^{n+\frac{1}{2}} \\ &\quad + \frac{2\Delta t}{r_{i+1}^2 - r_i^2} \left[-(E_{\theta_{i+1,j}}^{n+1} r_{i+1} - E_{\theta_{i,j}}^{n+1} r_i) \right], \end{aligned} \tag{17}$$

where Δt denotes the timestep, and the index n a value at time $t = n\Delta t$. In addition, the abbrevations $r_{i+\frac{1}{2}} = (r_{i+1} + r_i)/2$ and $z_{j+\frac{1}{2}} = (z_{j+1} + z_j)/2$ have been used.

The current $j_{\theta i,j}^{n+\frac{1}{2}}$ is obtained by adding the contributions of all the N_p particles in the system :

$$j_{\theta i,j}^{n+\frac{1}{2}} = \frac{2}{(r_{i+\frac{1}{2}}^2 - r_{i-\frac{1}{2}}^2)(z_{j+\frac{1}{2}} - z_{j-\frac{1}{2}})\Delta t} \sum_{N_p} Q_p \int_{t^n}^{t^{n+1}} dt \times \int\int dz\, r dr\, \Lambda_i(r)\, \Lambda_j(z)\, v_{\theta p}(t) \frac{\delta(r - r_p(t))}{r} \delta(z - z_p(t)). \quad (18)$$

Here, $r_p(t)$ and $z_p(t)$ describe the particle orbits, and $v_{\theta p}(t)$ is the θ-component of the velocity. The particle charge, Q_p, is the normalized version of the quantity defined in eq.(I.B.1).

The discrete equations governing the TE polarization being trivially charge conserving because $j_r = j_z = 0$, the following approximation for the integral in eq. (18) [8, sec. 15-5] can be used:

$$j_{\theta i,j}^{n+\frac{1}{2}} = \frac{2}{(r_{i+\frac{1}{2}}^2 - r_{i-\frac{1}{2}}^2)(z_{j+\frac{1}{2}} - z_{j-\frac{1}{2}})} \sum_{N_p} Q_p\, \Lambda_i(r_p^{n+\frac{1}{2}})\, \Lambda_j(z_p^{n+\frac{1}{2}})\, v_{\theta p}^{n+\frac{1}{2}}, \quad (19)$$

where $r_p^{n+\frac{1}{2}} = (r_p^{n+1} + r_p^n)/2$ and $z_p^{n+\frac{1}{2}} = (z_p^{n+1} + z_p^n)/2$.

3.2 Absorbing regions

The open boundaries at $z = 0$ and $z = L_z$ (fig. 1) are modelled with the perfectly matched layer technique [4] in which one uses absorbing layers of thickness L_{dl} and L_{dr}, on the left and on the right side of the cavity, respectively. The equations governing the TM polarization in these layers are given in eqs.(I.7-10) whereas the TE polarization satisfies the following normalized equations:

$$\frac{\partial E_{\theta r}}{\partial t} = -\frac{\partial B_z}{\partial r} - \frac{1}{2} j_\theta, \quad (20)$$

$$\frac{\partial E_{\theta z}}{\partial t} + \sigma_E E_{\theta z} = \frac{\partial B_r}{\partial z} - \frac{1}{2} j_\theta, \quad (21)$$

$$\frac{\partial B_r}{\partial t} + \sigma_B B_r = \frac{\partial (E_{\theta r} + E_{\theta z})}{\partial z}, \quad (22)$$

$$\frac{\partial B_z}{\partial t} = -\frac{1}{r}\frac{\partial}{\partial r}(r(E_{\theta r} + E_{\theta z})), \quad (23)$$

where $E_{\theta r}$, $E_{\theta z}$ are subcomponents of E_θ in the sense that $E_\theta = E_{\theta r} + E_{\theta z}$. The quantities σ_E and σ_B are normalized electric and magnetic conductivities [4], respectively. The current density in eqs (20) and (21) is obtained in exactly the same way as that in eqs. (5), using eq. (19).

According to Bérenger, the reflection coefficient for a plane wave incident on the interface at an angle ψ is given by

$$R(\psi) = \exp\left[-\frac{2}{3}\sigma_m \delta \cos\psi\right], \tag{24}$$

for a parabolic conductivity profile of the form

$$\sigma_E(\zeta) = \sigma_m \left(\frac{\zeta}{\delta}\right)^2, \tag{25}$$

where $\zeta = -z$, $\delta = L_{dl}$ in the left and $= z - L_z$, $\delta = L_{dr}$ in the right absorbing layer, respectively.

4 The computer code

The G2DEM structure follows the prescriptions of the Olympus system [9]. The core of the code is controlled by the subroutine STEPON, in which the parallel algorithm described in Section I.4 has been implemented. The variables used in G2DEM are mainly stored in common blocks, which are coded in separate files and inserted at compilation with include statements (table 2).

4.1 Input and output

The code starts by reading the variable NRESUM from the input channel 5. If NRESUM is equal to zero, the code starts a new run and reads all the parameters given in table 3. Otherwise, this is a restart run, and G2DEM reads only the variables denoted by a star in table 3 and the record files described below. At the end of the run, each processor saves the positions and momenta of its particles in the file "ATTP.MYPE.NREC", where MYPE is the processor number and NREC the record number read in input (table 3). The last processor (i.e. the processor with the highest number) saves the electromagnetic field in the file "ATTF.NPES.NREC", the Berenger subcomponents $E_{\theta r}$, (eq. 20), and $B_{\theta r}$, eq.(I.10), in the file "ATTBF.NPES.NREC", and history quantities in the file "ATTH.NPES.NREC". NPES is the number of processors required by the user.

Table 2
Include files

Include file	Title
COMBAS.ins	Olympus basic system parameters
COMDDP.ins	Olympus development and diagnostic parameters
pcombas.ins	Parallel parameters
PARAM	Dimensioning parameters
COMCON	Physical and normalization constants
COMDIA	Diagnostics quantities
COMFIL	Field parameters
COMNUM	Numerical parameters
COMOUT	Output control parameters
COMPAR	Particle parameters

The variables NTAVER, NZAVER and NFPRNT control the output produced by G2DEM on the output channel 6. NTAVER is the number of timesteps used for the Fourier transform of the following quantities : the normalized electromagnetic energy in the cavity, the normalized fluxes at both ends of the cavity, B_θ and E_θ both at six different points, in $r = 0, R_g$ and $z = \Delta z, L_z/2$, $L_z/2 - \Delta z$, where Δz is the mesh spacing along the cylinder axis.

G2DEM produces the time-averaged (over NZAVER steps) profiles along the cavity ($0 < z < L_z$) of the normalized energy, perpendicular and axial momentum components of the beam and of the spreads of these quantities. Also, one obtains every NFPRNT timesteps the longitudinal profile of the normalized Poynting flux $F(z)$ defined by :

$$F(z) = \int r dr (E_r B_\theta - E_\theta B_r). \tag{26}$$

At the end of the run the time histories of the following energy quantities can be displayed : the kinetic and total electromagnetic energies, the electric and magnetic energies separately and the fluxes, eq. (26), on both ends, $z = 0$ and $z = L_z$. The information for the two polarizations is given separately. Also displayed is the error in energy conservation.

Table 3
Input parameters

Name/length	Type	Purpose	Restart variable
NRESUM	I	Resume from record NRESUM if not equal to 0	*
NREC	I	Record number	*
LABEL1	IA	Label used to describe the run	*
LABEL2	IA	"	*
LABEL3	IA	"	*
LABEL4	IA	"	*
B0	R	External magnetic field, eq. (1)	
LMAG	I	External magnetic field option: (0:$\tau = 0$, 1:$\tau =$ DELTB)	
DELTB	R	τ [T/m], eq. (1)	
ALPHA	R	Velocity ratio, $v_\perp / v_{\|\|}$	
V0	R	Initial beam energy [kV]	
JCUR	R	Beam current [A]	
RG0M	R	R_{g0}, initial guiding center [m], eq.(8)	
DPP	R	$f_\perp$, initial spread in $P_\perp$, eq.(I.B.3)	
DPZ	R	$f_{\|\|}$, initial spread in $P_{\|\|}$, eq.(I.B.2)	
DRG	R	f_g, initial spread in guiding center, eq. (8)	
LZ	R	L_z, length of the cavity [m]	
NZ	I	Number of intervals between $z = 0$ and $z = L_z$. Must be a multiple of the number of processors	
NDL	I	Number of intervals for the absorbing layer on the left side	
NDR	I	Number of intervals for the absorbing layer on the right side. NDL + NZ + NDR must be a multiple of the number of processors	

Table 4
Input parameters

Name/length	Type	Purpose	Restart variable
REFLXL	R	$R(\psi = 0)$, reflection coefficient for the left absorbing layer, eq.(24)	
REFLXR	R	$R(\psi = 0)$,reflection coefficient for the right absorbing layer, eq.(24)	
NR(3)	RA	Number of intervals for each zone in the radial direction	
RBM(3)	RA	Radial coordinate of each zone in the radial direction	
NINJ	I	Number of particles by selected processors injected at each timestep	
NPEINJ	I	Number of processors selected to inject particles at each timestep NINJ * NEPINJ = N_{inj}, eq.(I.B.1)	
NCYC	I	Number of cyclotronic periods per timestep	
NLTM	I	equal to 1 if TM polarization is required	
NLTE	I	equal to 1 if TE polarization is required	
NTAVER	I	Number of steps used in FFT	*
NZAVER	I	Number of steps used in time average	*
NFPRNT	I	Frequency of print	*
NRUN	I	Maximum number of steps	*

4.2 Plots

The files ATTP, ATTF and ATTH are read by the code READB, which creates the plots of the phase space, of the longitudinal and radial profiles of the electromagnetic field components and the histories of diagnostic quantities (kinetic energy, field energy, etc.) using the Xgrafix package [10]. READB requires as input the number of processors (equal to 0 if G2DEM does not run on the T3D), and the record number NREC. Figure 2 shows the $z - P_z$ phase space at the end of the first test, produced by READB.

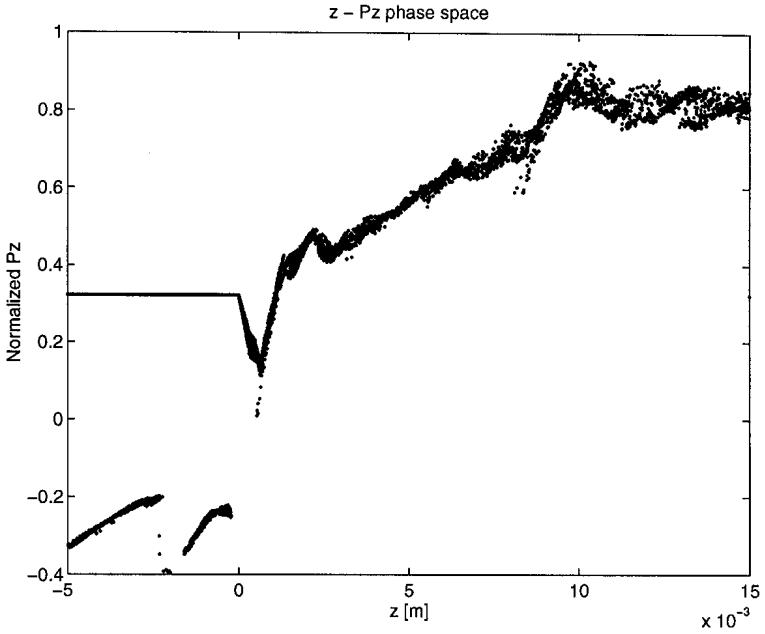

Fig. 2. $z - P_z$ phase space at $t = 0.35$ns

4.3 Tests

Two separate tests are provided for the TM and the TE polarizations. In the first case (TM), the code is run with a high-current electron beam which leads to the development of a virtual cathode shown in figure 2. In the second case (TE), the beam excites a TE_{02} mode which travels backwards towards the beam. Output from the first test is shown as *Test run output.* These two tests require less than 500 seconds each, on the CRAY T3D with 16 processors. In this case, practically all the time is spent in communication, the number of particles by processor being small ($\approx$ 500) [5].

Acknowledgement

This work was supported in part by the Swiss National Science Foundation, by Cray Research, Inc. within the framework of the Cray Research/EPFL Parallel Application Technology Program and by Thomson Tubes Electroniques. The computations were done on the Cray T3D massively parallel computer at EPFL, Lausanne.

References

[1] S. Alberti et al. Physics Fluids B2 (1990) 1654

[2] G. Soumagne,"Mesure de la fonction de distribution de vitesse du faisceau d'électrons d'un gyrotron quasi-optique", thèse N° 1390, Ecole Polytechnique de Lausanne, 1995.

[3] T. M. Tran et al., to be published

[4] J-P. Bérenger, Journal of Computational Physics 114 (1994) 185.

[5] G. Jost, T. M. Tran, K. Appert and S. Wüthrich, "Effects of electron-cyclotron instabilities on gyrotron beam quality", accepted for publication in Computer Physics Communications.

[6] J. D. Jackson, "Classical Electodynamics", John Wiley, New York, 1975

[7] J. W. Eastwood, Computer Physics Communications 64 (1991) 252.

[8] C. K. Birdsall, A. B. Langdon, "Plasma Physics via Computer Simulation", Adam Hilger, New York, 1991.

[9] K. V. Roberts, Computer Physics Communications 7 (1974) 237.

[10] V. Vahedi, J. P. Verboncoeur and P. Mirrashidi "Xgrafix library Version 1.1" University of California, Berkeley. Code and documentation are available through http://langmuir.eecs.berkeley.edu/pub/codes/Xgrafix.

Test run output

1

```
        OLYMPUS SYSTEM
        Universal VERSION I    12/05/94
        0.1 BASIC CONTROL DATA SET
        0.2 MODIFY BASIC DATA
      CURRENT DATE AND TIME    11/19/96    15:52:01
        0.3 ENTER RUN CONTROL
```

P R O G R A M G 2 D E M
****

G2DEM with 16 PEs

TM polarization only

Lz=0.01m Rw=5mm B0=3.8T no taper Rg = 3.mm

```
DATA
   B0     = 3.7999999999999998
   LMAG   = 0
   DELTB  = 0.
   ALPHA  = 1.5
   V0     = 80.
   JCUR   = 2500.
   RG0M   = 3.00000000000000006E-3
   DPP    = 0.
   DPZ    = 0.
   DRG    = 0.
   LZ     = 1.00000000000000002E-2
   NZ     = 32
   NDL    = 16
   NDR    = 16
   REFLXL = 1.E-20
   REFLXR = 1.E-20
   NR(1)  = 20
   NR(2)  = 36
   NR(3)  = 12
   RBM(0) = 0.
   RBM(1) = 2.50000000000000005E-3
   RBM(2) = 3.50000000000000007E-3
   RBM(3) = 5.0000000000000001E-3
   NINJ   = 1
   NPEINJ = 4
   NCYC   = 128
   NLTM   = 1
   NLTE   = 0
   NTAVER = 16384
   NZAVER = 512
   NFPRNT = 0
   NRUN   = 4097

END DATA
        1.5 SET AUXILLIARY VALUES


    GAMMA0  =  1.1566E+00
    PPERP0  =  4.8346E-01
    PPARR0  =  3.2231E-01
    TNORM   =  1.4962E-12
    DNORM   =  4.4856E-04
    ENORM   =  1.1392E+09
    BNORM   =  3.8000E+00
    QSIMUL  =  4.1635E-03


     CURRENT DATE AND TIME    11/19/96    15:52:01
     CPU TIME USED SO FAR =  1.6046E-01 SECS on PE  15
```

.
.
.

Time Average

NSTEP 1025 TIME 8.707E-11 DELT 5.677E-02

Min. and Max. of Ave. Dispersion of Gamma	0.000000E+00	8.322986E-03
Initial and final Ave. Gamma	8.225263E-01	0.000000E+00
Min. and Max. of Ave. Dispersion of Perp. P	0.000000E+00	3.669537E-02
Initial and final Ave Perp. P	3.438446E-01	0.000000E+00
Min. and Max. of Ave. Dispersion of Pz	0.000000E+00	3.606136E-02
Initial and final Ave Pz	2.297724E-01	0.000000E+00

	Z	Gamma	Spr. of Gam	Pperp	Spr. of Pperp	Pz	Spr. of Pz
Av. Pro.	1.084202E-19	8.225263E-01	3.340209E-03	3.438446E-01	1.498784E-02	2.297724E-01	1.645759E-02
Av. Pro.	3.125000E-04	7.259041E-01	8.043897E-03	3.026242E-01	3.669537E-02	2.099174E-01	3.107837E-02
Av. Pro.	6.250000E-04	6.428647E-01	8.322986E-03	2.652930E-01	3.626247E-02	2.070191E-01	3.606136E-02
Av. Pro.	9.375000E-04	5.765254E-01	5.702258E-03	2.335925E-01	2.054165E-02	2.105850E-01	3.113493E-02
Av. Pro.	1.250000E-03	5.186439E-01	4.884444E-03	2.057711E-01	1.381223E-02	2.118039E-01	2.402360E-02
Av. Pro.	1.562500E-03	4.638199E-01	4.947428E-03	1.805871E-01	1.734538E-02	2.073473E-01	1.807173E-02
Av. Pro.	1.875000E-03	4.113787E-01	4.502388E-03	1.571154E-01	1.786395E-02	1.979551E-01	1.364138E-02
Av. Pro.	2.187500E-03	3.589157E-01	3.860194E-03	1.343639E-01	1.571924E-02	1.835887E-01	1.040509E-02
Av. Pro.	2.500000E-03	3.092964E-01	3.014932E-03	1.135626E-01	1.185672E-02	1.666307E-01	7.766589E-03
Av. Pro.	2.812500E-03	2.574589E-01	2.261088E-03	9.270260E-02	7.920646E-03	1.450132E-01	5.769615E-03
Av. Pro.	3.125000E-03	2.061602E-01	1.649483E-03	7.276319E-02	4.787258E-03	1.207778E-01	4.168693E-03
Av. Pro.	3.437500E-03	1.555915E-01	1.115372E-03	5.390938E-02	2.548876E-03	9.441643E-02	2.701820E-03
Av. Pro.	3.750000E-03	1.027504E-01	5.261436E-04	3.499600E-02	1.367184E-03	6.414926E-02	1.208870E-03
Av. Pro.	4.062500E-03	4.773386E-02	1.040621E-04	1.599235E-02	4.882619E-04	3.035602E-02	2.212109E-04
Av. Pro.	4.375000E-03	0.000000E+00	0.000000E+00	0.000000E+00	0.000000E+00	0.000000E+00	0.000000E+00
Av. Pro.	4.687500E-03	0.000000E+00	0.000000E+00	0.000000E+00	0.000000E+00	0.000000E+00	0.000000E+00
Av. Pro.	5.000000E-03	0.000000E+00	0.000000E+00	0.000000E+00	0.000000E+00	0.000000E+00	0.000000E+00
Av. Pro.	5.312500E-03	0.000000E+00	0.000000E+00	0.000000E+00	0.000000E+00	0.000000E+00	0.000000E+00
Av. Pro.	5.625000E-03	0.000000E+00	0.000000E+00	0.000000E+00	0.000000E+00	0.000000E+00	0.000000E+00
Av. Pro.	5.937500E-03	0.000000E+00	0.000000E+00	0.000000E+00	0.000000E+00	0.000000E+00	0.000000E+00
Av. Pro.	6.250000E-03	0.000000E+00	0.000000E+00	0.000000E+00	0.000000E+00	0.000000E+00	0.000000E+00
Av. Pro.	6.562500E-03	0.000000E+00	0.000000E+00	0.000000E+00	0.000000E+00	0.000000E+00	0.000000E+00
Av. Pro.	6.875000E-03	0.000000E+00	0.000000E+00	0.000000E+00	0.000000E+00	0.000000E+00	0.000000E+00
Av. Pro.	7.187500E-03	0.000000E+00	0.000000E+00	0.000000E+00	0.000000E+00	0.000000E+00	0.000000E+00
Av. Pro.	7.500000E-03	0.000000E+00	0.000000E+00	0.000000E+00	0.000000E+00	0.000000E+00	0.000000E+00
Av. Pro.	7.812500E-03	0.000000E+00	0.000000E+00	0.000000E+00	0.000000E+00	0.000000E+00	0.000000E+00
Av. Pro.	8.125000E-03	0.000000E+00	0.000000E+00	0.000000E+00	0.000000E+00	0.000000E+00	0.000000E+00
Av. Pro.	8.437500E-03	0.000000E+00	0.000000E+00	0.000000E+00	0.000000E+00	0.000000E+00	0.000000E+00
Av. Pro.	8.750000E-03	0.000000E+00	0.000000E+00	0.000000E+00	0.000000E+00	0.000000E+00	0.000000E+00
Av. Pro.	9.062500E-03	0.000000E+00	0.000000E+00	0.000000E+00	0.000000E+00	0.000000E+00	0.000000E+00
Av. Pro.	9.375000E-03	0.000000E+00	0.000000E+00	0.000000E+00	0.000000E+00	0.000000E+00	0.000000E+00
Av. Pro.	9.687500E-03	0.000000E+00	0.000000E+00	0.000000E+00	0.000000E+00	0.000000E+00	0.000000E+00
Av. Pro.	1.000000E-02	0.000000E+00	0.000000E+00	0.000000E+00	0.000000E+00	0.000000E+00	0.000000E+00

CURRENT DATE AND TIME 11/19/96 15:52:21
CPU TIME USED SO FAR = 2.0414E+01 SECS on PE 15

.
.
.

Time Average

NSTEP 4097 TIME 3.480E-10 DELT 5.677E-02

Min. and Max. of Ave. Dispersion of Gamma	1.476377E-02	2.717372E-02
Initial and final Ave. Gamma	1.147165E+00	1.375499E+00
Min. and Max. of Ave. Dispersion of Perp. P	6.226663E-02	1.806226E-01
Initial and final Ave Perp. P	4.849521E-01	4.822386E-01
Min. and Max. of Ave. Dispersion of Pz	-6.290175E+00	2.694129E+00
Initial and final Ave Pz	1.956653E-01	8.077898E-01

	Z	Gamma	Spr. of Gam	Pperp	Spr. of Pperp	Pz	Spr. of Pz
Av. Pro.	1.084202E-19	1.147165E+00	1.476377E-02	4.849521E-01	6.226663E-02	1.956653E-01	2.694129E+00
Av. Pro.	3.125000E-04	1.129002E+00	2.344393E-02	4.873477E-01	1.141830E-01	1.452338E-01	-6.290175E+00
Av. Pro.	6.250000E-04	1.124122E+00	1.990643E-02	4.852182E-01	1.004339E-01	1.523323E-01	2.379519E-01
Av. Pro.	9.375000E-04	1.136030E+00	2.359761E-02	4.837100E-01	1.197791E-01	2.270958E-01	1.677017E-01
Av. Pro.	1.250000E-03	1.155340E+00	2.315432E-02	4.873487E-01	1.224881E-01	3.034942E-01	9.844317E-02
Av. Pro.	1.562500E-03	1.171318E+00	2.099453E-02	4.850430E-01	1.131888E-01	3.625493E-01	7.185680E-02
Av. Pro.	1.875000E-03	1.187035E+00	2.054272E-02	4.836159E-01	1.129704E-01	4.111379E-01	5.896688E-02
Av. Pro.	2.187500E-03	1.202049E+00	2.081551E-02	4.835891E-01	1.210551E-01	4.515060E-01	4.775826E-02
Av. Pro.	2.500000E-03	1.214691E+00	2.293435E-02	4.824591E-01	1.357987E-01	4.843967E-01	4.143908E-02
Av. Pro.	2.812500E-03	1.226367E+00	2.263303E-02	4.829739E-01	1.354583E-01	5.127722E-01	3.758319E-02
Av. Pro.	3.125000E-03	1.237593E+00	2.106316E-02	4.858849E-01	1.259186E-01	5.371665E-01	3.470368E-02
Av. Pro.	3.437500E-03	1.246745E+00	2.024044E-02	4.868435E-01	1.191968E-01	5.577458E-01	3.291095E-02
Av. Pro.	3.750000E-03	1.253303E+00	1.994043E-02	4.846532E-01	1.172311E-01	5.745078E-01	3.186448E-02
Av. Pro.	4.062500E-03	1.259476E+00	1.991930E-02	4.832230E-01	1.206322E-01	5.891100E-01	3.082579E-02
Av. Pro.	4.375000E-03	1.265486E+00	1.962543E-02	4.828978E-01	1.235379E-01	6.021809E-01	2.814652E-02
Av. Pro.	4.687500E-03	1.272656E+00	1.963811E-02	4.862150E-01	1.241752E-01	6.146416E-01	2.758529E-02
Av. Pro.	5.000000E-03	1.278900E+00	2.015976E-02	4.883745E-01	1.240306E-01	6.259020E-01	3.034742E-02
Av. Pro.	5.312500E-03	1.283673E+00	2.038640E-02	4.871529E-01	1.218718E-01	6.366659E-01	3.270285E-02
Av. Pro.	5.625000E-03	1.288371E+00	2.051978E-02	4.854103E-01	1.238036E-01	6.474613E-01	3.332037E-02
Av. Pro.	5.937500E-03	1.293531E+00	2.119770E-02	4.850393E-01	1.336571E-01	6.577775E-01	3.164906E-02
Av. Pro.	6.250000E-03	1.299078E+00	2.221891E-02	4.866386E-01	1.428722E-01	6.671924E-01	3.011830E-02

Av. Pro.	6.562500E-03	1.304207E+00	2.309035E-02	4.884200E-01	1.469350E-01	6.756328E-01	3.191482E-02
Av. Pro.	6.875000E-03	1.308943E+00	2.344493E-02	4.900589E-01	1.465806E-01	6.834524E-01	3.515671E-02
Av. Pro.	7.187500E-03	1.312788E+00	2.342965E-02	4.896375E-01	1.443233E-01	6.911596E-01	3.762745E-02
Av. Pro.	7.500000E-03	1.316716E+00	2.401650E-02	4.880301E-01	1.474017E-01	6.996487E-01	3.810786E-02
Av. Pro.	7.812500E-03	1.320649E+00	2.483823E-02	4.857548E-01	1.574986E-01	7.082598E-01	3.615749E-02
Av. Pro.	8.125000E-03	1.325219E+00	2.565294E-02	4.837239E-01	1.687267E-01	7.176612E-01	3.320677E-02
Av. Pro.	8.437500E-03	1.331400E+00	2.600689E-02	4.828571E-01	1.744552E-01	7.293301E-01	3.119617E-02
Av. Pro.	8.750000E-03	1.338007E+00	2.626520E-02	4.810276E-01	1.771892E-01	7.424786E-01	3.064188E-02
Av. Pro.	9.062500E-03	1.346071E+00	2.672291E-02	4.807178E-01	1.789671E-01	7.571871E-01	3.058089E-02
Av. Pro.	9.375000E-03	1.355281E+00	2.717372E-02	4.815000E-01	1.806226E-01	7.730877E-01	3.080820E-02
Av. Pro.	9.687500E-03	1.365546E+00	2.711613E-02	4.817803E-01	1.801161E-01	7.910220E-01	3.112792E-02
Av. Pro.	1.000000E-02	1.375499E+00	2.626142E-02	4.822386E-01	1.774435E-01	8.077898E-01	2.857509E-02

CURRENT DATE AND TIME 11/19/96 15:54:01
CPU TIME USED SO FAR = 1.2162E+02 SECS on PE 15

History Arrays

Nhist	Time [s]	NPART	NPOUT	WEM	WE	WB	Left Flux	Right Flux	EcinErr	En. Bal.
1	0.000E+00	0	0	0.000E+00	0.000E+00	0.000E+00	0.000E+00	0.000E+00	0.000E+00	0.000E+00
101	8.494E-12	400	0	2.882E-27	2.543E-27	3.394E-28	1.377E-26	1.543-137	0.000E+00	7.036E-28
201	1.699E-11	800	0	5.678E-17	3.918E-17	1.760E-17	1.118E-16	3.949E-81	0.000E+00	1.032E-17
301	2.548E-11	1200	0	3.028E-11	2.001E-11	1.027E-11	4.780E-11	8.900E-52	0.000E+00	4.793E-12
401	3.398E-11	1600	0	1.249E-06	8.015E-07	4.472E-07	1.562E-06	7.921E-34	0.000E+00	1.678E-07
501	4.247E-11	2000	0	2.908E-03	1.857E-03	1.051E-03	2.669E-03	5.922E-23	0.000E+00	3.105E-04
601	5.097E-11	2400	0	4.432E-01	2.982E-01	1.450E-01	2.690E-01	5.289E-16	0.000E+00	3.566E-02
701	5.946E-11	2800	0	9.271E+00	7.128E+00	2.143E+00	3.685E+00	7.400E-11	0.000E+00	6.380E-01
801	6.796E-11	3200	0	4.259E+01	3.531E+01	7.281E+00	1.010E+01	8.249E-07	6.934E+01	2.251E+00
901	7.645E-11	3600	0	8.491E+01	7.360E+01	1.131E+01	1.231E+01	5.229E-04	1.563E+02	3.145E+00
1001	8.494E-11	4000	0	1.263E+02	1.109E+02	1.532E+01	1.382E+01	1.198E-02	2.529E+02	3.518E+00
1101	9.344E-11	4400	0	1.802E+02	1.552E+02	2.506E+01	1.698E+01	2.709E-03	3.497E+02	4.273E+00
1201	1.019E-10	4800	0	2.500E+02	2.113E+02	3.877E+01	1.974E+01	-4.886E-03	4.483E+02	5.065E+00
1301	1.104E-10	5200	0	3.151E+02	2.685E+02	4.660E+01	1.989E+01	2.307E-01	5.588E+02	5.621E+00
1401	1.189E-10	5600	0	3.569E+02	3.112E+02	4.563E+01	1.910E+01	1.372E+00	6.478E+02	6.370E+00
1501	1.274E-10	6000	0	3.908E+02	3.447E+02	4.607E+01	2.071E+01	2.797E+00	6.909E+02	7.243E+00
1601	1.359E-10	6400	0	4.366E+02	3.814E+02	5.517E+01	2.198E+01	3.842E+00	7.195E+02	9.313E+00
1701	1.444E-10	6716	3	4.646E+02	3.957E+02	6.890E+01	2.226E+01	5.510E+00	7.231E+02	1.240E+01
1801	1.529E-10	6972	3	4.728E+02	3.969E+02	7.586E+01	2.230E+01	6.556E+00	7.483E+02	1.140E+01
1901	1.614E-10	7192	2	4.669E+02	3.961E+02	7.089E+01	1.765E+01	6.176E+00	7.818E+02	1.006E+01
2001	1.699E-10	7385	3	4.708E+02	4.043E+02	6.647E+01	1.734E+01	5.483E+00	7.906E+02	9.353E+00
2101	1.784E-10	7552	3	4.745E+02	4.084E+02	6.609E+01	1.629E+01	5.839E+00	7.936E+02	1.014E+01
2201	1.869E-10	7682	4	4.622E+02	3.902E+02	7.198E+01	1.729E+01	9.267E+00	7.743E+02	1.370E+01
2301	1.954E-10	7771	3	4.511E+02	3.753E+02	7.572E+01	2.074E+01	1.134E+01	7.366E+02	1.400E+01
2401	2.039E-10	7834	4	4.562E+02	3.836E+02	7.260E+01	2.265E+01	6.646E+00	7.068E+02	1.244E+01
2501	2.124E-10	7870	0	4.825E+02	4.143E+02	6.821E+01	2.100E+01	5.700E+00	7.314E+02	1.228E+01
2601	2.209E-10	7863	5	4.749E+02	4.127E+02	6.217E+01	1.524E+01	4.950E+00	7.598E+02	1.201E+01
2701	2.294E-10	7835	2	4.486E+02	3.863E+02	6.231E+01	1.344E+01	6.267E+00	7.772E+02	1.486E+01
2801	2.378E-10	7874	3	4.281E+02	3.634E+02	6.470E+01	1.608E+01	6.814E+00	7.529E+02	1.492E+01
2901	2.463E-10	7901	7	4.413E+02	3.668E+02	7.450E+01	2.370E+01	7.952E+00	7.297E+02	1.430E+01
3001	2.548E-10	7926	5	4.837E+02	4.084E+02	7.527E+01	2.517E+01	6.940E+00	7.109E+02	1.488E+01
3101	2.633E-10	7934	5	4.854E+02	4.195E+02	6.593E+01	1.666E+01	8.748E+00	7.368E+02	1.711E+01
3201	2.718E-10	7902	5	4.388E+02	3.793E+02	5.953E+01	1.189E+01	6.609E+00	7.477E+02	1.505E+01
3301	2.803E-10	7885	4	4.090E+02	3.536E+02	5.540E+01	1.286E+01	4.844E+00	7.674E+02	1.351E+01
3401	2.888E-10	7925	4	4.166E+02	3.508E+02	6.582E+01	1.883E+01	6.108E+00	7.706E+02	1.608E+01
3501	2.973E-10	7933	3	4.580E+02	3.841E+02	7.391E+01	2.451E+01	8.251E+00	6.888E+02	1.870E+01
3601	3.058E-10	7924	10	4.707E+02	3.985E+02	7.214E+01	2.129E+01	8.982E+00	7.091E+02	1.795E+01
3701	3.143E-10	7903	6	4.434E+02	3.783E+02	6.505E+01	1.383E+01	6.986E+00	7.351E+02	1.622E+01
3801	3.228E-10	7823	8	4.069E+02	3.484E+02	5.849E+01	1.146E+01	4.587E+00	7.519E+02	1.472E+01
3901	3.313E-10	7900	1	3.998E+02	3.451E+02	5.468E+01	1.392E+01	3.602E+00	7.416E+02	1.758E+01
4001	3.398E-10	7879	4	4.143E+02	3.549E+02	5.942E+01	2.003E+01	6.817E+00	7.276E+02	1.964E+01

4.2 TERMINATE THE RUN
RECORD = 1
NSTEP = 4097

CURRENT DATE AND TIME 11/19/96 15:54:11
CPU TIME USED SO FAR = 1.3197E+02 SECS on PE 15